Fokker-Planck analysis of short-pulse laser heating in the hot-spot-model approximation

P. E. Pulsifer and K. G. Whitney
Radiation Hydrodynamics Branch, Plasma Physics Division, Naval Research Laboratory, Washington, D.C. 20375-5346
(Received 20 June 1994)

The electron distribution function in high-power, short-pulse, laser-produced plasmas is predicted to be significantly non-Maxwellian during plasma heating. This directly affects radiation production and ionized-state populations and alters the plasma heating rates and transport coefficients. Here we numerically solve a time-dependent Fokker-Planck equation to calculate electron energy distributions for a near-critical-density selenium plasma irradiated by a 2 ps pulse width KrF laser with powers between 5×10^{14} and 7×10^{16} W cm^{-2}. Distributions are calculated locally, with plasma heating treated as in the hot-spot model [K. G. Whitney and J. Davis, J. App. Phys. **45**, 5294 (1974)], which focuses on a small, stationary volume element heated by inverse bremsstrahlung and cooled by heat conduction and electron-ion energy exchange. Inelastic electron-ion collisions, previously seen to have little influence on the distribution, and bremsstrahlung cooling, which is negligible in magnitude, are not included. Intense, long-pulse inverse-bremsstrahlung heating produces non-Maxwellian distributions of a well-known, depleted-tail form [A. B. Langdon, Phys. Rev. Lett. **44**, 575 (1980)]. We show that in the present case, because of short time scales and high plasma density, these do not accurately represent the electron distribution. We obtain actual distributions both during and several picoseconds after the laser pulse and determine the resulting effect on the laser absorption coefficient, heat conductivity, and electron-ion coupling rate as a function of the peak intensity of the laser pulse. It is found that the non-Maxwellian distribution results in greater heating; a reduction in the laser absorption coefficient is more than balanced by the reduction in thermal conductivity. Electron-ion coupling is generally unaffected ($<10\%$) by the non-Maxwellian distribution. These effects increase as a function of laser intensity.

PACS number(s): 52.50.Jm, 52.40.Nk, 52.25.Fi, 42.55.Vc

I. INTRODUCTION

Recent technological advances in short-pulse-width (<10 ps), high-power ($>10^{15}$ W cm^{-2}) lasers have sharpened interest in laser-plasma interactions [1,2]. Such tabletop terawatt (T^3) lasers open up new areas of high-field physics and allow rapid heating of dense plasmas. Short-pulse lasers have been proposed as drivers for recombination x-ray lasers, using optical field ionization in low-density plasmas [3] as well as collisional ionization with rapid cooling in near-critical density plasmas [4], a situation similar to that considered here. They have also been used to irradiate solid-density targets and generate bright, ultrafast x-ray pulses [5]. In all laser-plasma interaction experiments, the form of the electron energy distribution is very important. Radiation from the plasma is directly affected by the shape of the distribution function [6,7] and such radiation effects could be used to infer the distribution function spectroscopically [8]. More importantly, because the collisional heating rate and transport coefficients are determined largely by the electron distribution, the electron temperatures and so the x-ray emission or x-ray laser gain in dense plasmas are dependent on the distribution shape. This too could provide diagnostic information about plasma conditions; for example, the quality of amplified spontaneous emission could signal the generation of nonequilibrium distributions in an irradiated high-Z plasma [4].

The short pulse widths and high powers of T^3 lasers ensure that the electron distribution function will be non-Maxwellian both during and shortly after heating. For strong inverse-bremsstrahlung heating at moderate densities on a nanosecond time scale, the distribution has been analytically approximated [9,10], but for short picosecond pulse widths, for high densities, or when strong turbulence is present, numerical solutions to the kinetic equation are required. Here we present a model of laser heating in a near-critical-density, highly ionized plasma. Unlike other studies [8,11], we are primarily concerned with the effect of non-Maxwellian distributions on the local transport and hydrodynamics and not with the details of spatial gradients; such an analysis for long-pulse heating is found in Ref. [10].

Our focus in this work is on the evolution of the isotropic part of the electron distribution in energy (or velocity) space, at or near the critical surface of the plasma, where maximum laser absorption can occur. Energy balance in this small region involves heating by resonant inverse bremsstrahlung and cooling by electron conduction and collisions with ions. These processes compete with isotropizing electron-electron collisions to determine the distribution function shape. The electron distribution is calculated locally from the Fokker-Planck equation in velocity space and the (possibly flux-limited) heat conduction is proportional to the local gradient in plasma temperature as described by the hot-spot model [12], a hydrodynamic description of a plasma volume element in which motion is ignored. This approximation is particularly apt in this case because the relevant time scales, the pulse width and ionization times, are so short. As we

shall show, the kinetic model developed is term-by-term consistent with, and thus extends, the hot-spot-model hydrodynamic results.

One important application for the results given here is demonstrated in Ref. [4], where "hot-spot"-based calculations showed that, beyond laser intensities of a few times 10^{15} W cm^{-2}, a selenium plasma would ionize quickly into the neonlike ionization stage, where large population inversions between the $J=0$, $3p$ states and the $J=1$, $3s$ states would be generated (gain coefficients larger than, and possibly much larger than, 100 cm^{-1}). This earlier work studied the interaction of a small, motionless plasma volume element near the critical surface of a KrF laser with short (2 ps full width $1/e$ maximum) KrF heating pulses, which ranged in peak intensity from 5×10^{14} to 7×10^{16} W cm^{-2}. A set of rate equations, nonlinearly coupled to the hot-spot hydrodynamic equations, was solved to determine the (nonequilibrium) picosecond ionization response of the plasma. However, the underlying assumption of these calculations was that the electrons had a Maxwellian distribution, which produced the familiar set of rate equations and energy equations that are widely used to describe plasma dynamics. It was noted that this assumption is incorrect, and in this paper we will begin to quantify the degree to which it breaks down as a function of laser intensity as well as to assess the impact of short-pulse generated non-Maxwellian electrons on the hydrodynamic equations.

This paper is structured as follows. The kinetics model is derived in Sec. II and its connection to the hydrodynamic hot-spot model is discussed in Sec. III. In Sec IV the non-Maxwellian solutions to the kinetic model are presented and compared to previously used analytic distributions. The non-Maxwellian distributions produce sizable corrections to the laser absorption rate, heat conduction rate, and electron-ion heat transfer rate. These are calculated and their dependence on laser intensity is investigated. Finally, implications of the results are discussed in Sec. V. For numerical expressions in this paper, hybrid units are employed unless otherwise indicated: that is, CGS units are used for most quantities, temperature and other energies are in eV, powers is in watts, and laser wavelength is in micrometers.

II. THE KINETIC EQUATION

The model plasma consists of electrons with mass m_e, charge $-e$ ($e>0$), and density n_e and of ions with mass m_i, charge Ze, and density n_i. The driving laser pulse has frequency ω and period $2\pi/\omega=3.34\lambda$ fs, where the wavelength λ is in micrometers. The laser pulse width τ_p for T^3 lasers can be of order 100 fs–10 ps. Because of plasma oscillations, laser absorption is enhanced at the critical surface, where the electron density is

$$n_c=1.11\times10^{21}\lambda^{-2}\ \text{cm}^{-3}\ . \tag{1}$$

The electron quiver motion in the laser field is $v(t)=v_0\cos\omega t$. If the laser intensity is I (in W cm^{-2}), then the peak electron quiver energy $\epsilon_q\equiv\frac{1}{2}m_e v_0^2$ is

$$\epsilon_q=1.87\times10^{-13}\lambda^2 I\ \text{eV}\ , \tag{2}$$

which can be many times the thermal energy. Inverse-bremsstrahlung heating is important when $\epsilon_q>T_e$. On the other hand, the theory given here is only valid for nonrelativistic electron energy $I\ll10^{19}\lambda^{-2}$ W cm^{-2}.

In a stationary plasma, the Boltzmann equation for the electron distribution function $f(v)$ (normalized to n_e) has the form

$$\frac{\partial f}{\partial t}+\mathbf{v}\cdot\nabla f+\mathbf{a}\cdot\nabla_v f=C_{\text{el}}+C_{\text{inel}} \tag{3}$$

with small-angle elastic collisions C_{el} described by a Landau collision term [13] and inelastic electron-ion collisions represented by C_{inel}. The electron acceleration $\mathbf{a}(t)$ comes solely from the laser pulse, although the plasma-frequency resonance at the critical density will be included later phenomenologically.

We employ a Cartesian-tensor expansion for the distribution [13], retaining, as is commonly done, only the isotropic and vector terms

$$f(\mathbf{v})=f_0(v)+\hat{\mathbf{v}}\cdot\mathbf{f}_1(v)\ . \tag{4}$$

This approximation is often used even when the anisotropy is not very small [11,14]. Using the expansion, assuming the ions to be in an isotropic Maxwellian distribution, and neglecting the effect of electron-electron collisions on $\mathbf{f}_1(v)$, we obtain two coupled equations

$$\frac{\partial f_0}{\partial t}+\frac{v}{3}\nabla\cdot\mathbf{f}_1+\frac{1}{3v^2}\frac{\partial}{\partial v}[v^2\mathbf{a}\cdot\mathbf{f}_1]=C_{\text{FP}}+C_{ei}\ , \tag{5}$$

$$\frac{\partial\mathbf{f}_1}{\partial t}+\nu_{ei}\mathbf{f}_1=-v\nabla f_0-\mathbf{a}\frac{\partial f_0}{\partial v}\ . \tag{6}$$

The Fokker-Planck elastic collision term C_{FP} and the electron-ion elastic collision term C_{ei} are taken from Ref. [13]. The contribution of inelastic collisions is neglected because of their comparatively weak effect on the distribution function, even when inelastic energy losses are relatively important [15,16]. Because of the neglect of inelastic collisions, all the terms in Eq. (5) manifestly conserve particle number. Energy is conserved only by the Fokker-Planck term.

The isotropic distribution determines the average electron energy and so the temperature

$$T_e=\frac{2}{3n_e}\int[\tfrac{1}{2}m_e v^2]f_0(v)d^3v\ . \tag{7}$$

The thermal velocity is then defined to be

$$v_{\text{th}}=\sqrt{2T_e/m_e}\ . \tag{8}$$

The frequency of elastic collisions between particles of species a and b is

$$\nu_{ab}(v)=\frac{4\pi Z_a^2Z_b^2e^4n_b}{m_a^2v^3}\ln\Lambda\ , \tag{9}$$

where v is the relative velocity and $\ln\Lambda$ is the Coulomb logarithm [13]. The distribution f_0 relaxes to a Maxwellian in roughly the time $\nu_{ee}^{-1}(v_{\text{th}})$. The distribution $\mathbf{f}_1$ is determined largely by electron-ion collisions because $\nu_{ei}/\nu_{ee}=Z\gg1$. The characteristic time scale of the important plasma heating and cooling processes is the in-

verse electron-ion collision frequency. By convention, this time is defined as $\tau_e \equiv 3\sqrt{\pi}/4\nu_{ei}(v_{\rm th})$ or

$$\tau_e = 0.3440 \frac{T_e^{3/2}}{(Zn_e/10^{18})\ln\Lambda} \text{ ps} . \tag{10}$$

We now introduce a dimensionless energy variable and distribution function. Using dimensionless variables makes the analysis of the distribution function more transparent and increases computational power by not binding the calculation of the distribution function to any fixed energy grid. A normalized time variable is not used because the relevant time scales (the collision times) vary with density and temperature changes and normalization results in no simplification. At any given time, however, the contemporary collision time τ_e can be used as a convenient time measure. Accordingly, we define

$$\epsilon = (v/v_{\rm th})^2 , \tag{11}$$

$$f(\epsilon) = (v_{\rm th}^3/n_e) f_0(v) , \tag{12}$$

where the normalized distribution $f(\epsilon)$ is distinguished by its argument from the dimensional $f_0(v)$. The normalized Maxwellian distribution $f^M(\epsilon)$ is given by

$$f^M(\epsilon) = \frac{1}{\pi^{3/2}} \exp(-\epsilon) . \tag{13}$$

The invariant moments of the normalized distribution function are, in terms of the density of states function $g_e(\epsilon) = 2\pi\epsilon^{1/2}$,

$$\int_0^\infty f(\epsilon,t) g_e(\epsilon) d\epsilon = 1 , \tag{14}$$

$$\int_0^\infty f(\epsilon,t) \epsilon g_e(\epsilon) d\epsilon = \tfrac{3}{2} . \tag{15}$$

Because of the normalization, the distribution function $f(\epsilon)$ has no direct information about changes in density or temperature. Lacking inelastic terms, the kinetic equation cannot supply information on density changes; however, the time evolution of the energy can be determined separately and self-consistently from the kinetic equations.

The solution to Eq. (6) produces inverse-bremsstrahlung [9] and heat conduction [17] terms in the f_0 equation Eq. (5). These terms are obtained by separating $\mathbf{f}_1$ into rapidly and slowly varying components, respectively, and then averaging the heating from the rapidly varying component over a laser period. In terms of the normalized variables, and after substituting for $\mathbf{f}_1$ from Eq. (6), the kinetic equation Eq. (5) becomes

$$\frac{\partial f}{\partial t} - \frac{1}{T_e}\frac{dT_e}{dt}\frac{1}{\sqrt{\epsilon}}\frac{\partial}{\partial\epsilon}(\epsilon^{3/2} f) = C_{\rm FP} + C_{\rm IB} - C_{ei} - C_{\rm cond} . \tag{16}$$

The second term on the left-hand side of Eq. (16) preserves the energy moment Eq. (15) of the time-evolving distribution function. The Fokker-Planck electron-electron collision term in dimensionless form is

$$C_{\rm FP} = \frac{3\sqrt{\pi}}{4Z\tau_e}\frac{4\pi}{\sqrt{\epsilon}} \left\{ f(\epsilon) \int_0^\epsilon f(\epsilon') \epsilon'^{1/2} d\epsilon' + \frac{2}{3}\frac{\partial f}{\partial\epsilon} \left[\int_0^\epsilon f(\epsilon') \epsilon'^{3/2} d\epsilon' + \epsilon^{3/2} \int_\epsilon^\infty f(\epsilon') d\epsilon' \right] \right\} . \tag{17}$$

The inverse-bremsstrahlung heating term is obtained by averaging the work done by the laser electric field over one period [9]:

$$C_{\rm IB} = \frac{\sqrt{\pi}}{2\tau_e} \frac{v_0^2/v_{\rm th}^2}{\sqrt{1-n/n_c}} \frac{1}{\sqrt{\epsilon}} \frac{\partial}{\partial\epsilon} \left[g(\epsilon) \frac{\partial f}{\partial\epsilon} \right] , \tag{18}$$

where

$$g(\epsilon) \equiv \frac{1}{1+(\epsilon_0/\epsilon)^3} , \tag{19}$$

$$\epsilon_0 \equiv \left[\frac{3\sqrt{\pi}}{4\omega\tau_e} \right]^{2/3} . \tag{20}$$

The expression for $C_{\rm IB}$ includes a resonance factor $(1-n/n_c)^{-1/2}$, which comes from the coupling between the laser and plasma oscillations at the critical surface [18].

The electron-ion elastic collision term, which arises from the ion contribution to $C_{\rm el}$ in Eq. (3), is [13]

$$C_{ei} = -\frac{3\sqrt{\pi}}{2\tau_e}\frac{m_e}{m_i}\frac{1}{\sqrt{\epsilon}}\frac{\partial}{\partial\epsilon} \left[I\left(\frac{m_i}{m_e}\epsilon \right) \left[f(\epsilon) + \frac{T_i}{T_e}\frac{\partial f}{\partial\epsilon} \right] \right] , \tag{21}$$

where the function $I(x)$ comes from the ion distribution and ensures that C_{ei} conserves particle number:

$$I(x) \equiv \Phi(x) - x\Phi'(x) , \tag{22}$$

$$\Phi(x) \equiv \frac{2}{\sqrt{\pi}} \int_0^x e^{-y^2} dy . \tag{23}$$

Although $I(0)=0$, the large magnitude of m_i/m_e allows us to replace $I(x)$ by $I(\infty)=1$ for most calculations.

The conduction cooling term derives from the $\nabla\cdot\mathbf{f}_1$ term in Eq. (5). Assuming there is no static current, it is [17]

$$C_{\rm cond} = -\frac{1}{3}\nabla\cdot \left[\frac{4\tau_e}{3\sqrt{\pi}} v_{\rm th}^2 \epsilon^{5/2} \times \left\{ \left[\frac{\langle\epsilon^3\rangle}{3\langle\epsilon^2\rangle}\frac{\partial f}{\partial\epsilon} + f \right] \frac{1}{n}\nabla n + \left[\left[\frac{5\langle\epsilon^3\rangle}{6\langle\epsilon^2\rangle} - \epsilon \right] \frac{\partial f}{\partial\epsilon} - \frac{3}{2} f \right] \times \frac{1}{T}\nabla T \right\} \right] , \tag{24}$$

where

$$\langle \epsilon^m \rangle \equiv 4\pi \int_0^\infty f(\epsilon)\epsilon^m d\epsilon \ . \tag{25}$$

The density-gradient term in Eq. (24) vanishes for a Maxwellian distribution and we will omit it, assuming in any event that temperature gradients are much more important on the short time scale.

III. THE HOT-SPOT MODEL

The hot-spot model [12] is a hydrodynamic model that can be used to obtain rapid, physically accurate estimates of the magnitudes of heating and cooling terms. In addition, applications of this model have included an extensive treatment of atomic excitation and deexcitation collisions and so could accurately determine the plasma electron density and the excited state populations [4]. In principle, the hot-spot-model equations of motion for n_e and T_e are derivable from the two lowest moments of the f_0 kinetic equation. The kinetic model developed above lacks inelastic collisions and so cannot determine the density variation, but, as we shall show, the hot-spot-model energy equation is obtained by taking the energy moment of the corresponding kinetic terms in Eq. (16). As with most hydrodynamic models, the hot-spot energy terms have been calculated with a Maxwellian distribution. The kinetic theory presented here will allow these terms to be generalized to non-Maxwellian plasmas.

The hot-spot-model energy equation is found by taking the energy moment of Eq. (16), remembering that the density and energy moments of the normalized distribution [Eqs. (14) and (15)] are constant. The resultant equation for $(1/T_e)dT_e/dt$ can be multiplied by $p_e = n_e T_e$ to obtain an equation for the electron energy density $E = \frac{3}{2} n_e T_e$:

$$\left[\frac{\partial E}{\partial t}\right]_{\text{hot spot}} = \tfrac{3}{2} n_e T_e \int_0^\infty [C_{\text{FP}} + C_{\text{IB}} - C_{ei} - C_{\text{cond}}] \times \epsilon g_e(\epsilon) d\epsilon \tag{26}$$

$$= S_e - Q_{ei} - Q_h \ . \tag{27}$$

The integration of C_{FP} gives zero. The important physical processes are inverse bremsstrahlung S_e, elastic collisions with ions Q_{ei}, and electron thermal conduction Q_h. The terms omitted from Eq. (27) that have previously been included in the hot-spot model are inelastic collisions and bremsstrahlung cooling. We have argued that the former should not significantly alter the distribution function and hot-spot energy calculations [4] have shown that inelastic collisions are not a major factor in the early time energy balance for this problem; a simple calculation [19] shows that, for this problem, bremsstrahlung is many orders of magnitude smaller than any other term, even at high temperature.

The magnitudes of the hot-spot energy terms are found by carrying out the integrations in Eq. (26) for a Maxwellian distribution. To obtain the usual inverse-bremsstrahlung heating term [18], we use C_{IB} from Eq. (18), also assuming that $\epsilon_0 \approx 0$, so that $g(\epsilon) \approx 1$. The result is

$$S_e = \left[\frac{n_e}{3.4\times 10^{18}}\right]^2 \frac{Z \ln\Lambda}{T_e^{3/2}} \frac{\lambda^2 I}{\sqrt{1-n_e/n_c}} \ \text{W cm}^{-3} \ . \tag{28}$$

The assumption that $\epsilon_0 = 0$, or that the electron-ion collision frequency is much less than the laser frequency, is not always well satisfied in dense plasmas. Numerically, this parameter is

$$\epsilon_0 = \frac{1.73}{T_e} \left[\frac{n_e}{n_c} \frac{Z \ln\Lambda}{\lambda}\right]^{2/3} , \tag{29}$$

which can approach one near critical density, especially for highly charged plasmas. As we shall see, even a small value of ϵ_0 can reduce the heating rate.

Electron cooling from elastic collisions with ions can be calculated by integrating C_{ei} from Eq. (21) with a Maxwellian distribution, according to Eq. (26), giving the heat transfer rate [20]

$$Q_{ei} = \frac{3 n_e}{\tau_e} \frac{m_e}{m_i} (T_e - T_i) \ . \tag{30}$$

In the hot-spot model, this is the sole heating process for the ions, so that the energy density in the ions changes as

$$\frac{\partial}{\partial t}\left[\frac{3}{2} n_i T_i\right] = Q_{ei} \ . \tag{31}$$

Conduction cooling is determined by spatial temperature (and density) gradients. These are approximated in the hot-spot model by assuming that laser energy deposition occurs within a uniform stationary sphere of radius r at the laser focus. The radius r is chosen to be comparable to an average value of the inverse-bremsstrahlung absorption length [18]

$$\lambda_{\text{abs}}^{\text{IB}} = \frac{1.11\times 10^{16} T_e^{3/2}}{Z n_e \ln\Lambda} \frac{\sqrt{1-n_e/n_c}}{n_e/n_c} \ \text{cm} \ . \tag{32}$$

The heat flux from the hot spot is taken to be equal to its average over the surface

$$\nabla \cdot \mathbf{q} \approx \frac{1}{\Delta V} \int_{\Delta V} \nabla \cdot \mathbf{q} \, dV = \frac{3}{r} q \cdot \hat{\mathbf{r}} \ . \tag{33}$$

In addition, the temperature gradient is assumed to have a uniform scale length l_e, so that we can write

$$\frac{1}{T_e} \hat{\mathbf{r}} \cdot \nabla T_e \approx \frac{1}{l_e} \ . \tag{34}$$

Conduction losses due to the temperature gradient can thus be written in terms of the parameters r and l_e. If we omit terms proportional to ∇n_e, the heat conduction term in Eq. (24) becomes

$$C_{\text{cond}} = -\frac{4\tau_e}{3\sqrt{\pi}} \frac{v_{\text{th}}^2}{r l_e} \epsilon^{5/2} \left[\left[\frac{5\langle\epsilon^3\rangle}{6\langle\epsilon^2\rangle} - \epsilon\right] \frac{\partial f}{\partial \epsilon} - \frac{3}{2} f\right] . \tag{35}$$

The local heat flow is conventionally expressed as

$$Q_h = \nabla \cdot [\kappa_e \nabla T_e] \ , \tag{36}$$

where κ_e is the thermal conductivity. Taking the energy moment of $C_{\rm cond}$ as prescribed in Eq. (26), we obtain the standard [17,20] expression for the heat conductivity of an equilibrium Lorentz plasma

$$\kappa_e = \frac{128}{3\pi}\frac{n_e T_e \tau_e}{m_e} . \tag{37}$$

The expression for the temperature-gradient heat flow in a Lorentz plasma is then

$$Q_h = \frac{3.95\times 10^3}{r l_e}\frac{T_e^{7/2}}{Z\ln\Lambda}\ W\,\mathrm{cm}^{-3} . \tag{38}$$

The effect of a non-Maxwellian distribution on heat conduction will be expressed through the resultant modification of κ_e. Conduction cooling becomes rapidly (and anomalously) more important as the electron temperature increases and so the conduction term is usually limited [4] to some fraction of the free-streaming heat flow $n_e v_{\rm th} T_e$. This flux-limiting procedure was not needed, however, for the calculations presented in this paper.

In this paper, our procedure for solving Eq. (16) is to treat the fluid quantities n_e, T_e, and T_i as time-dependent parameters whose values are imported from the calculations described in Ref. [4]. This procedure allows us to determine the resultant time-dependent non-Maxwellian distributions and the magnitude of the modifications to heating and cooling rates that they engender as a first step in an iterative procedure. As we shall show, compensating reductions in heating and cooling terms that are produced by these non-Maxwellian distributions limit the magnitude of the changes these terms produce in T_e. Thus it appears that the iteration of hydrodynamic and kinetic equations initiated here should converge fairly rapidly to a self-consistent solution of the full set of model equations.

The time dependence of n_e is determined in Ref. [4] by solving a self-consistently coupled set of rate equations for the available states [12]. The atomic states in the model have population N_μ, defined such that

$$n_e = \sum_\mu Z_\mu N_\mu .$$

Ionization, recombination, excitation, and deexcitation cause transitions between states μ and ν during the pulse, at the rates [4] $W_{\mu\nu}(n_e, T_e)$, so that

$$\frac{dN_\mu}{dt} = \sum_\nu W_{\mu\nu} N_\nu .$$

The net change in total internal energy is

$$\frac{d}{dt}\sum_\mu E_\mu N_\mu = Q_i - R_i , \tag{39}$$

where Q_i is the net collisional excitation rate from electrons and R_i is the rate of energy loss by line and radiative recombination processes. Because of the absence of these terms from Eq. (27), both radiation losses and the buildup of $\sum_\mu E_\mu N_\mu$ are neglected in our kinetic equation. The calculations of Ref. [4] show this to be a second-order omission.

The non-Maxwellian distributions generated during the laser pulse produce different heating and cooling rates from those of S_e, Q_{ei}, and Q_h. Using the kinetic model, we can calculate corrections to these rates. If the Maxwellian rates are factored out of the collision terms, they become

$$C_{\rm IB} \equiv (S_e/p_e) C^0_{\rm IB} , \tag{40}$$

$$C_{ei} \equiv (Q_{ei}/p_e) C^0_{ei} , \tag{41}$$

$$C_{\rm cond} \equiv (Q_h/p_e) C^0_{\rm cond} , \tag{42}$$

which defines

$$C^0_{\rm IB} = \frac{\sqrt{\pi}}{2}\frac{1}{\sqrt{\epsilon}}\frac{\partial}{\partial\epsilon}\left[g(\epsilon)\frac{\partial f}{\partial\epsilon}\right] , \tag{43}$$

$$C^0_{ei} = -\frac{\sqrt{\pi}}{2}\frac{1}{\sqrt{\epsilon}}\frac{\partial}{\partial\epsilon}\left[I\left[\frac{m_i}{m_e}\epsilon\right]\frac{T_e f(\epsilon) + T_i \partial f/\partial\epsilon}{T_i - T_e}\right] , \tag{44}$$

$$C^0_{\rm cond} = -\frac{\sqrt{\pi}}{48}\epsilon^{5/2}\left[\left[\frac{5\langle\epsilon^3\rangle}{6\langle\epsilon^2\rangle} - \epsilon\right]\frac{\partial f}{\partial\epsilon} - \frac{3}{2} f\right] . \tag{45}$$

Integrations over these quantities define non-Maxwellian correction factors $\alpha_{\rm IB}$, α_{ei}, and α_h to the inverse-Bremsstrahlung absorption rate, the electron-ion transfer rate, and the heat conductivity, respectively, e.g.,

$$\alpha_{\rm IB}(t) \equiv \int_0^\infty C^0_{\rm IB}(\epsilon, t)\epsilon g_e(\epsilon) d\epsilon . \tag{46}$$

For Maxwellian distributions, $\alpha_{\rm IB} = \alpha_{ei} = \alpha_h = 1$. Using these correction factors, we can rewrite the hot-spot-model energy balance equation Eq. (27) with an arbitrary electron distribution as

$$\left[\frac{dE}{dt}\right]_{\rm hot\ spot} = \alpha_{\rm IB} S_e - \alpha_{ei} Q_{ei} - \alpha_h Q_h . \tag{47}$$

IV. RESULTS

The α correction factors derived above can be evaluated analytically for a family of distribution functions that are frequently used to approximate non-Maxwellian distributions in long-pulse laser-heated plasmas. These functions have the form [9,21]

$$f_m(\epsilon) = \frac{a_m}{\epsilon_m^{3/2}} e^{-(\epsilon/\epsilon_m)^{m/2}} , \tag{48}$$

where

$$a_m = \frac{m}{4\pi\Gamma(3/m)} , \tag{49}$$

$$\epsilon_m = \frac{3\Gamma(3/m)}{2\Gamma(5/m)} . \tag{50}$$

The function $f_2(\epsilon)$ is a Maxwellian, an exact solution to the equation $C_{\rm FP} = 0$. The function $f_5(\epsilon)$ is an exact self-similar solution to Eq. (16) with $C_{\rm IB}$ the sole source term, if it is assumed that $\epsilon_0 = 0$ and that the laser intensity is constant [9]. More generally, $f_m(\epsilon)$, with $2 \le m \le 5$,

can be a good approximation to the distributions calculated from Eq. (16) if the important source terms are C_{FP} and C_{IB}. In this case, the value of m can be phenomenologically determined [22] from the laser intensity and electron temperature. For the short-pulse problem considered here, the $f_m(\epsilon)$ functions are not as good an approximation to the electron distribution because of the picosecond time scale, the importance of the conduction term, and the fact that ϵ_0 is not always negligible.

The $f_m(\epsilon)$ distributions can be used to obtain analytic expressions for the non-Maxwellian α correction factors. These expressions, with m related to the laser intensity as in Ref. [22], can then be compared with the correction factors derived from solutions to Eq. (16) to assess the utility of using the $f_m(\epsilon)$ as approximate distributions for short-pulse heated plasmas. Taking $f(\epsilon)$ to be given by $f_m(\epsilon)$ in Eqs. (43)–(45) produces the following correction factors for the inverse-bremsstrahlung heating rate, the elastic electron-ion heat transfer rate, and the conduction cooling rate:

$$\alpha_{IB}^{(m)} \approx \pi^{3/2} \frac{a_m}{\epsilon_m^{3/2}} e^{-(\epsilon_0/1.26\epsilon_m)^m} , \tag{51}$$

$$\alpha_{ei}^{(m)} = \pi^{3/2} \frac{a_m}{\epsilon_m^{3/2}} \frac{T_e[2\epsilon_m/m]\Gamma(2/m) - T_i}{T_e - T_i} , \tag{52}$$

$$\alpha_h^{(m)} = \frac{\sqrt{\pi}}{96} \frac{\epsilon_m^{7/2}}{\Gamma(3/m)} \left[\frac{7}{2}\Gamma(10/m) - \frac{10}{3} \frac{\Gamma(8/m)^2}{\Gamma(6/m)} \right] . \tag{53}$$

In the expression for $\alpha_{IB}^{(m)}$, valid for small ϵ_0, the initial factor gives the modification to the inverse-bremsstrahlung heating rate due to the non-Maxwellian distribution $f_m(\epsilon)$, while the exponential factor approximates the reduction in heating rate when $\epsilon_0 > 0$ (high electron density, low temperature). Inverse-bremsstrahlung heating is always reduced by these non-Maxwellian distributions, as was shown by Langdon [9]. As m increases from 2 to 5, $\alpha_{IB}^{(m)}$ monotonically decreases to about 0.4. The electron-ion factor $\alpha_{ei}^{(m)}$ is generally slightly less than one, except when the electron and ion temperatures are nearly equal. When $T_e < 5T_i$, the non-Maxwellian distribution enhances electron-ion coupling, reflecting the fact that heat can flow from non-Maxwellian electrons to Maxwellian ions even when they are at the same temperature. The electron-ion transfer rate is quite small in this case, however, even though the factor α_{ei} may be very large for $T_i \approx T_e$. Finally, the conduction cooling rate can be significantly reduced with these non-Maxwellian distributions: α_h monotonically declines with increasing m to a minimum of about 0.25 when $m = 5$. These results have been obtained and discussed by Mora and Yahi [23], who derived an expression equivalent to Eq. (53).

To calculate the distribution functions arising under strong short-pulse laser heating, we numerically solved the Fokker-Planck equation Eq. (16), using a time-dependent, implicit scheme. Energy conservation by the Fokker-Planck term C_{FP} was checked with a predictor-corrector iteration to ensure proper energy balance. In the remainder of this section, we will first discuss the time dependence of the electron distribution and its consequences and then show how these results vary with laser intensity. The latter discussion is relevant to x-ray laser gain calculations reported earlier [4]: The laser intensities chosen here are the same as those used in Ref. [4], so a direct connection may be made with this work.

As in Ref. [4], our calculations involve a preformed selenium plasma irradiated by a KrF laser pulse ($\lambda = 0.248$ μm), with a Gaussian shape and a full width $1/e$ maximum pulse width of 2 ps. Eight calculations corresponding to eight different peak laser intensities were carried out. These intensities are listed in Table I. The electron distribution was assumed initially in a Maxwellian equilibrium at about 10 eV, with an ion density of 6×10^{20} cm^{-3}; this ion density is such that, after heating for the duration of the pulse, the electron density is close to, but remains less than, the critical density $n_c = 1.8 \times 10^{22}$ cm^{-3}.

The Gaussian laser pulse profile used in these calculations is shown in Fig. 1. An identical profile was used in all runs, with the peak at 3 ps and the magnitude of the peak varying. The distribution function evolution for heating with a peak intensity of 3.2×10^{16} W cm^{-3} is shown in Fig. 2, where we have plotted the calculated distribution relative to a Maxwellian:

$$\gamma(t) \equiv f(\epsilon,t)/f^M(\epsilon) . \tag{54}$$

Like the f_m distributions, the calculated distribution tail is depleted as the laser pulse intensifies and m correspondingly increases, and is repopulated when the pulse ends.

The effect of the non-Maxwellian distribution on the plasma hydrodynamics is shown in Figs. 3, 4, and 5, where the correction factors α_{IB}, α_{ei}, and α_h, respectively, are plotted as solid lines for the case of peak intensity 3.2×10^{16} W cm^{-2}. In these figures, the dotted lines are the correction factors for the distribution $f_m(\epsilon)$, obtained from Eqs. (51)–(53), with m given by the formula of Alaterre, Matte, and Lamoureaux [22]. The value of m as a function of time for each of the peak intensities in Table I is shown as a family of curves in Fig. 6. The calculated distributions produce inverse-bremsstrahlung heating rates and conduction cooling rates significantly different from both Maxwellian and $f_m(\epsilon)$ distributions, while the electron-ion transfer rate is close to its Maxwellian value. The discrepancy between the f_m distribution and the actual-distribution curves largely reflects the transient nature of the plasma response and shows the importance

TABLE I. Peak laser intensities.

Case	Peak intensity (W cm^{-2})
1	4.9×10^{14}
2	9.9×10^{14}
3	2.0×10^{15}
4	3.9×10^{15}
5	7.9×10^{15}
6	1.6×10^{16}
7	3.2×10^{16}
8	6.3×10^{16}

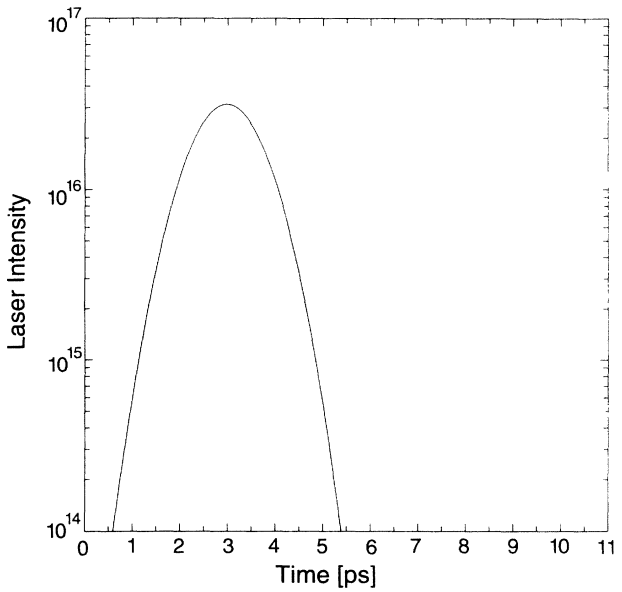

FIG. 1. The (Gaussian) laser pulse profile as a function of time. The peak intensity, but not the pulse shape, varies for the different examples used in the paper.

of obtaining the actual distribution.

A significant additional effect in dense or turbulent plasmas is the modification in the inverse-bremsstrahlung heating rate when the electron-ion collision frequency is comparable to the laser frequency. This modification enters the calculation as a finite value of ϵ_0 and its effect

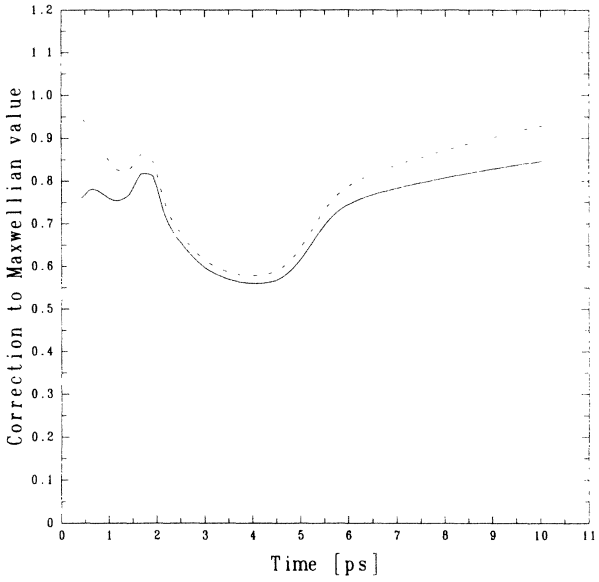

FIG. 3. The correction factor α_{IB} for inverse-bremsstrahlung heating rate as a function of time for the numerically determined distribution (solid line) and the equivalent self-similar distribution $f_m(\epsilon)$, with m as shown in Fig. 6 (dotted line). The peak laser intensity was 3.2×10^{16} W cm^{-2}. The solid line is the ratio of the actual heating rate, with ϵ_0 nonzero (cf. Fig. 7), to the classical rate in Eq. (28), which assumes $\epsilon_0=0$. The dashed line shows the correction factor attributed solely to the non-Maxwellian distribution; for this curve the nonzero ϵ_0 was used to compute the Maxwellian heating rate in the denominator.

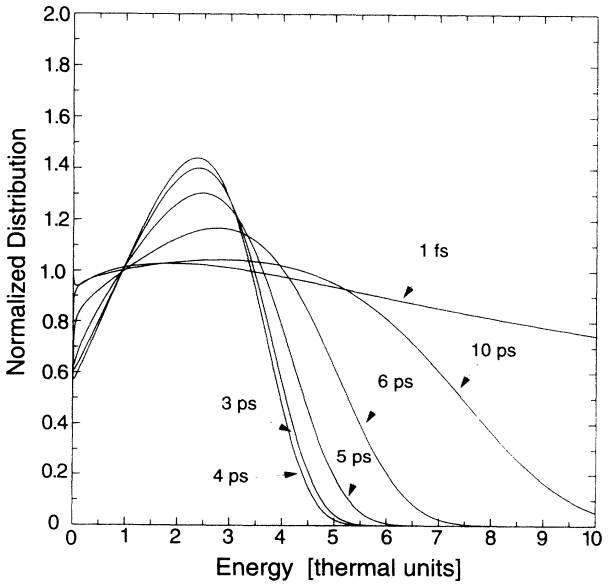

FIG. 2. The electron distribution function shape at different times. The curves are snapshots at time 1 fs and 3, 4, 5, 6, and 10 ps, as marked. The peak laser intensity was 3.2×10^{16} W cm^{-3}, reached at 3 ps. The abscissa is the normalized energy variable ϵ and the ordinate is γ, the ratio of the distribution to a Maxwellian distribution.

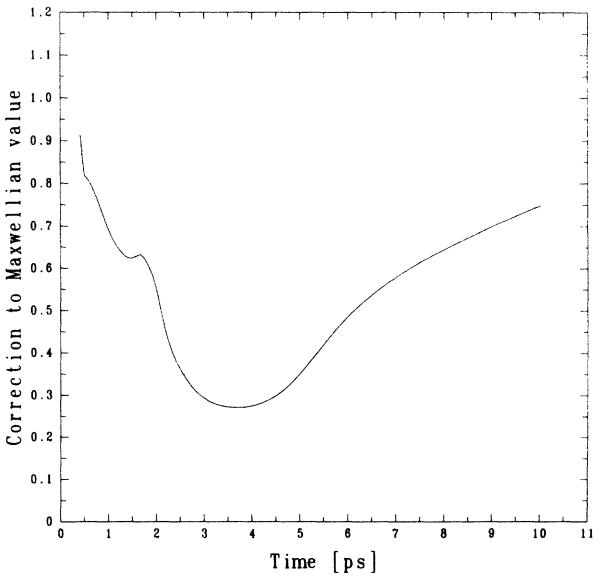

FIG. 4. The correction factor α_h for conduction cooling as a function of time for the numerically determined distribution (solid line) and the equivalent self-similar distribution $f_m(\epsilon)$, with m as shown in Fig. 6 (dotted line). The peak laser intensity was 3.2×10^{16} W cm^{-2}.

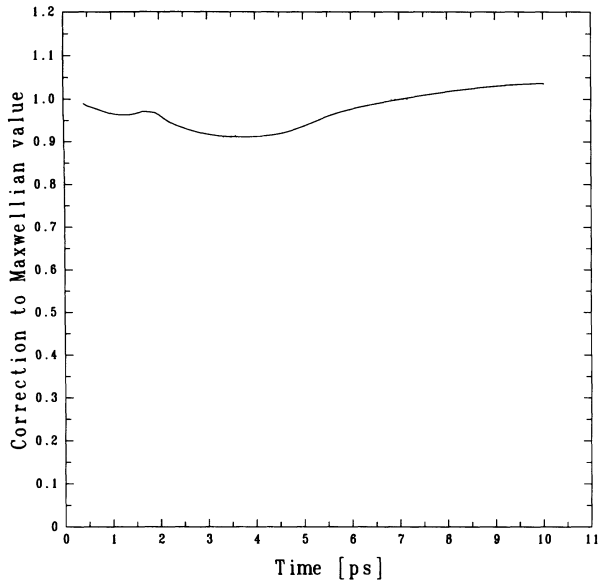

FIG. 5. The correction factor α_{ei} for electron-ion energy exchange as a function of time for the numerically determined distribution (solid line) and the equivalent self-similar distribution $f_m(\epsilon)$, with m as shown in Fig. 6 (dotted line). The peak laser intensity was 3.2×10^{16} W cm^{-2}.

on the heating rate of the $f_m(\epsilon)$ distribution is approximated by the exponential factor in Eq. (51); similar corrections will occur with other distributions. The correction factor shown by the solid line in Fig. 3 includes the $\epsilon_0\neq0$ modification as well as the effect of the non-Maxwellian distribution. To isolate the effect of the distribution alone on the heating rate, one can calculate the nonzero ϵ_0 modification α_{IB}^M to the Maxwellian rate Eq. (28) by substituting $f^M(\epsilon)$ in Eqs. (43) and (46). Dividing α_{IB} by α_{IB}^M gives the correction due solely to the distribution function, which is shown in Fig. 3 as a dashed line. This latter correction approaches one at the initial time, but the solid line correction, including also the effect of finite ϵ_0, gives a more accurate heating rate. The assumption that ϵ_0 is small underlies the derivation of C_{IB}, since it must be true that $\epsilon_0<1$ in order to time average the heating term after solving Eq. (6). This condition is not violated in our calculation, but finite ϵ_0 effects are important. As Eq. (29) shows, the value of ϵ_0 is proportional for fixed ion density to $Z^{4/3}T_e^{-1}$; the actual values of ϵ_0 are plotted in Fig. 7 as a family of curves for each of the intensities given in Table I.

The importance of non-Maxwellian effects as a function of laser intensity can be seen in Figs. 8 and 9, where the calculated correction factors are plotted for each of the intensities given in Table I. The inverse-bremsstrahlung heating rate and conduction cooling rate are both increasingly limited by the distribution as laser intensity increases. These effects compensate to some degree in the plasma energy balance and the net effect of non-Maxwellian distributions is to change the local plasma energetics more than the local temperature history. This is seen in Fig. 10, which is a plot of the plasma temperature as a function of time, determined by the hydrodynamic hot-spot model [4] of Eq. (47), with correction factors either set to unity (Maxwellian distribution) or to the time-varying values determined by this work. The temperature of the non-Maxwellian plasma is somewhat

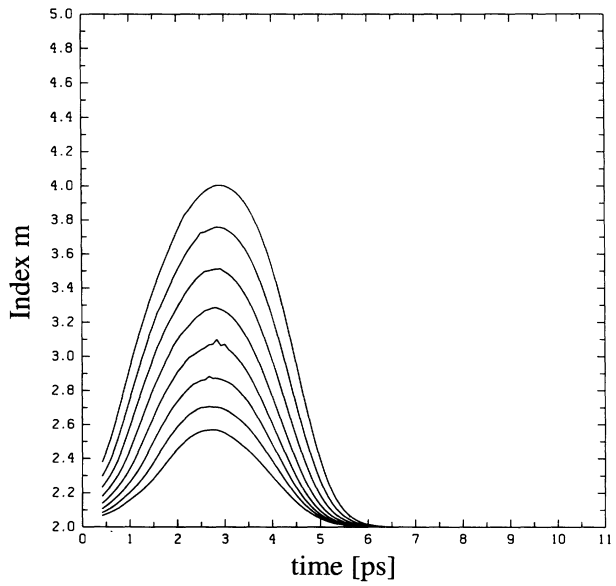

FIG. 6. The value of m, which gives the best-fit $f_m(\epsilon)$ distribution for the current laser intensity and electron temperature, from the formula of Alaterre, Matte, and Lamoureaux [22]. The values are plotted as a function of time for each of the runs with peak intensities given in Table I. The lowest curve is for the lowest peak intensity (case 1) and each higher curve corresponds to a higher peak intensity.

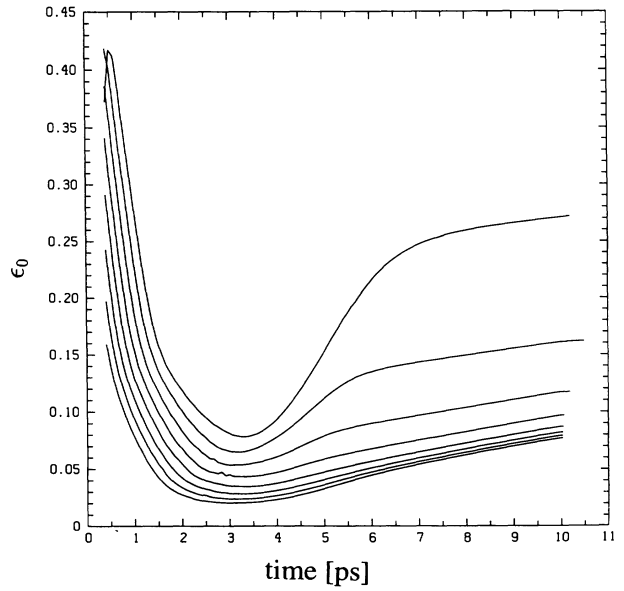

FIG. 7. The actual values of $\epsilon_0=(3\sqrt{\pi}/4\omega\tau_e)^{2/3}$ as a function of time, a separate curve for each of the intensities given in Table I. The highest curve corresponds to the lowest peak intensity (case 1) and successively lower curves correspond to higher peak intensities.

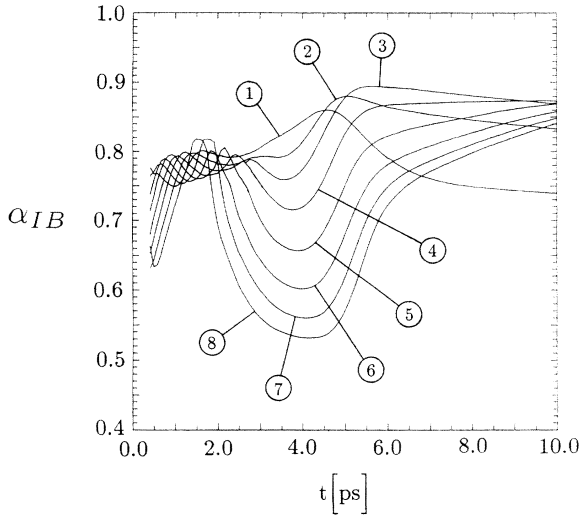

FIG. 8. The calculated correction factors α_{IB} for inverse-bremsstrahlung heating rate as a function of time for each of the intensities given in Table I.

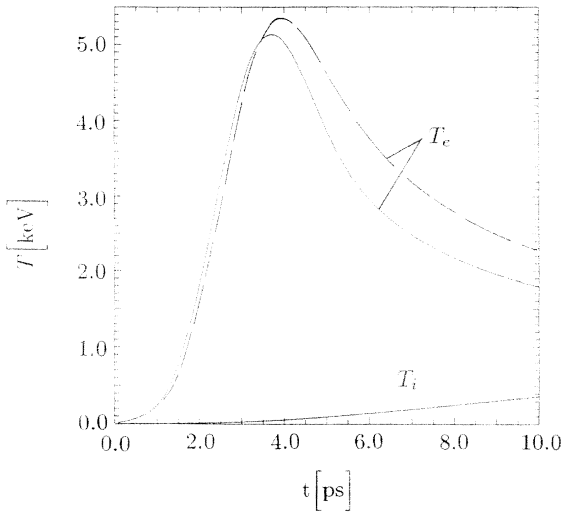

FIG. 10. The electron and ion temperatures as a function of time, as computed with the hydrodynamic hot-spot model [4], using Maxwellian heating and cooling rates (solid line) and using the correction factors computed here (dotted line).

higher than the Maxwellian one. The laser energy deposition was much smaller in the non-Maxwellian plasma, which may have important experimental consequences: 570 J/μg of laser energy was deposited in the uncorrected calculation, but only 348 J/μg was deposited in the corrected calculation.

In addition to its effect on the heating rates, the shape of the distribution function will be important in determining radiative output from the plasma. In short-pulse heating, ionization is delayed relative to the laser pulse, resulting in population inversions and possible amplified spontaneous emission that is similarly delayed. Thus the distribution shape after the pulse, during the generation of radiation, could be particularly important. In the hydrodynamic calculations of Ref. [4], for example, the peak of the laser pulse occurred at 3 ps, but the selenium plasma was not ionized into the L shell until 4 ps and the gain coefficient due to the resulting population inversions peaked in value at 5.5 ps. With the depleted-tail distributions produced by laser heating, the time to collisionally ionize the plasma could be further delayed. To illustrate both the maximum extent of deviation from a Maxwellian and the post-pulse relaxation towards a Maxwellian, we show calculated electron distribution functions for each of the peak laser intensities in Table I, at two times of particular interest for the x-ray laser gain calculations of Ref. [4]. In Fig. 11, the electron distributions are shown at 3 ps, the time of peak intensity. At this time, the plasma has shown significant heating and ionization

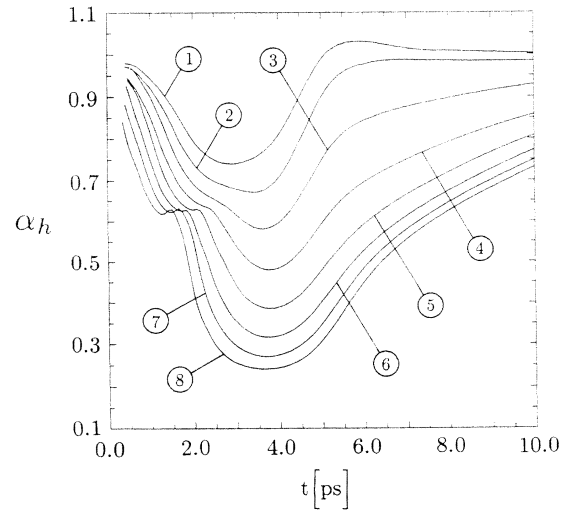

FIG. 9. The calculated correction factors α_h for conduction cooling as a function of time for each of the intensities given in Table I.

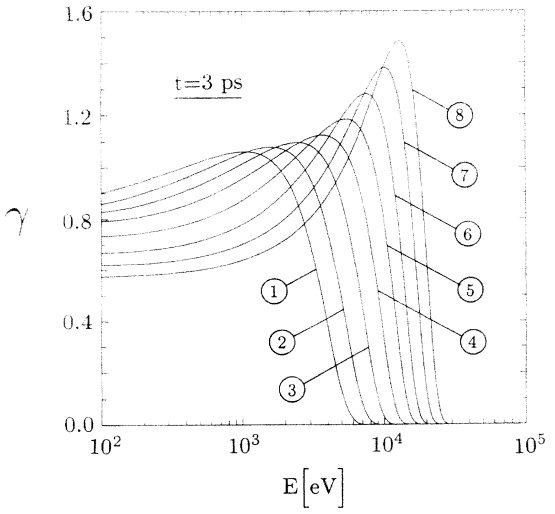

FIG. 11. The electron distribution as a function of energy, at 3 ps, the time of peak laser intensity. The abscissa is the electron energy in eV (log scale) and the ordinate is the ratio of the actual distribution to a Maxwellian.

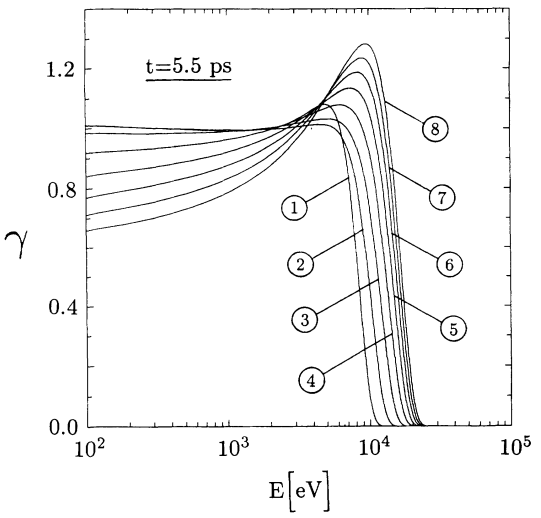

FIG. 12. The electron distribution as a function of energy, at 5.5 ps, when the maximum gain is predicted in Ref. [4]. The abscissa is the electron energy in eV (log scale) and the ordinate is the ratio of the actual distribution to a Maxwellian.

and the distribution is strongly non-Maxwellian. In Fig. 12 the same set of electron distributions are shown at 5.5 ps, the time when maximum gain is predicted. While some relaxation of the distributions towards a Maxwellian has occurred, the deviations appear to be large enough to have a measurable effect on the gain calculations.

V. CONCLUSIONS

We have formulated a kinetic description of plasma heating by short-pulse, high-power lasers and used it to calculate modifications to the local plasma heating and heat flow that result from the generation of non-Maxwellian electron distributions. The distributions are driven to be non-Maxwellian primarily by strong inverse-bremsstrahlung heating (such that $Z\epsilon_q/T_e \gg 1$ during most of the pulse) and conduction cooling (which is initially small, but grows in importance as $T_e^{7/2}$). Plasma heating initially occurs on a subpicosecond time scale for all peak intensities in Table I, so that electron temperatures of several hundred eV are attained within 2 ps (see Fig. 10); at these temperatures, even at critical density, the collisional times (e.g., τ_e) characteristic of the distribution function response to heating and cooling, or to collisional relaxation, are greater than the laser-pulse width. Thus the short-pulse generated distributions should be quite different from those found in strong long-pulse heating.

Non-Maxwellian distributions measurably alter the plasma heating and cooling terms. The principal effect is on the thermal conductivity, which is reduced for the highest laser intensity in Table I to as low as one-quarter its Maxwellian value. The inverse-bremsstrahlung heating rate is also reduced to as low as one-half its Maxwellian value for the highest-intensity case. The overall result of the non-Maxwellian distributions is to produce somewhat hotter electrons than predicted by the Maxwellian hydrodynamics. Non-Maxwellian generation acts like a flux limiter for laser heating and reduces the requirements on the laser-pulse energy needed to heat a plasma to a given temperature.

The ion heating rate from elastic collisions is only slightly reduced or enhanced, by up to about 10%. This is potentially good diagnostics news, since the observation of unexpectedly high ion temperatures (and large Doppler linewidths) in short-pulse heating experiments might therefore be attributable to the presence of ion-acoustic microturbulence at the critical surface that is generated by the laser absorption processes [24].

We have compared the calculated distributions from our model with the functions $f_m(\epsilon)$ that have been used in the past to model laser-heated electron distributions, with m determined from laser intensity and electron temperature as specified in Ref. [22]. Using the modifications to heating and cooling rates as the criterion, we find that the f_m distributions with these values of m do not give accurate values of these rates in the short-pulse cases considered. This is due to the short time scales and high densities in the present problem: the short time scale gives the distribution little time to equilibrate or approach self-similar behavior, while the high electron-ion collision frequency effectively shifts the focus of the laser heating so the lowest-energy electrons are not the most rapidly heated. Microturbulence, if present, would increase the effective collisionality [24] and further alter the distribution.

The kinetic model presented here is well integrated with the hot-spot hydrodynamic model and the hot-spot calculations of Ref. [4] were used to determine the electron density and temperature variations required in the kinetics calculations. This procedure allowed us to account for inelastic processes without explicitly including them in the kinetic model. In principle, Eq. (16) should be solved self-consistently with Eq. (47) or, more rigorously, with the complete hot-spot equations of Ref. [4], including the inelastic terms in the rate equations. Because of the difficulty of simultaneously solving the hydrodynamic and kinetic equations, our approach here was to initiate an iterative solution, which our results suggest should converge after a small number of iterations. Thus the solutions in this paper to Eq. (16) are based on the Maxwellian-distribution calculations described in Ref. [4]. When the α correction factors of Figs. 3–5 are incorporated through Eq. (47), then the hot-spot-model equations of Ref. [4] will change according to the calculations described in this paper. These changes to the hydrodynamics calculations are evident in the hotter "corrected" temperature curve in Fig. 10. Note also that the collisional excitation and ionization rates used in the rate equations will be changed by the non-Maxwellian distributions.

The recent observation of neonlike x-ray spectra from experiments [25] using 35 mJ, 1 ps KrF pulses to heat copper plasmas have provided some experimental support for the basic ionization predictions of the model calculations of Ref. [4], which were used to drive our kinetics calculations. Radiation measurements [8], e.g., of satellite lines, will be needed to experimentally investigate the predictions made here about the evolution of the dis-

tribution function and its dependence on the peak intensity of the laser pulse.

Our kinetics model employed a local description of heat transport and ignored nonlocal effects. In short gradient length plasmas, nonlocal transport can also be important in determining the distribution function at each point, and our kinetic model could be readily extended to study nonlocal transport along the same lines others have followed [14,26].

ACKNOWLEDGMENT

This work was supported by the Ballistic Missile Defense Office/DFI.

[1] G. Mourou and D. Umstadter, Phys. Fluids **4**, 2315 (1992).
[2] *Femtosecond to Nanosecond High-Intensity Lasers and Applications,* edited by E. M. Campbell (SPIE, Bellingham, WA 1990).
[3] N. H. Burnett and P. B. Corkum, J. Opt. Soc. Am. B **6**, 1195 (1989); P. Amendt, D. C. Eder, and S. C. Wilks, Phys. Rev. Lett. **66**, 2589 (1991); P. Pulsifer, J. P. Apruzese, J. Davis, and P. Kepple, Phys. Rev. A **49**, 3958 (1994).
[4] K. G. Whitney, A. Dasgupta, and P. E. Pulsifer, Phys. Rev. E **50**, 468 (1994).
[5] M. M. Murnane, H. C. Kapteyn, M. D. Rosen, and R. W. Falcone, Science **251**, 531 (1991); H. Chen, B. Soom, B. Yaakobi, S. Uchida, and D. D. Meyerhofer, Phys. Rev. Lett. **70**, 3431 (1993).
[6] J. P. Matte, M. Lamoureaux, C. Möller, R. Y. Yin, J. Delettrez, J. Virmont, and T. W. Johnston, Plasma Phys. Contr. Fusion **30**, 1665 (1988).
[7] Michèle Lamoureaux, Adv. At. Mol. Opt. Phys. **31**, 233 (1993).
[8] J. P. Matte, J. C. Kieffer, S. Ethier, and M. Chaker, Phys. Rev. Lett. **72**, 1208 (1994); A. Dasgupta, K. G. Whitney, and P. E. Pulsifer, Bull. Am. Phys. Soc. **39**, 1205 (1994).
[9] A. B. Langdon, Phys. Rev. Lett. **44**, 575 (1980).
[10] Roger D. Jones and K. Lee, Phys. Fluids **25**, 2307 (1982).
[11] L. Drska, J. Limpouch, and R. Liska, Laser Part. Beams **10**, 461 (1992).
[12] K. G. Whitney and J. Davis, J. Appl. Phys. **45**, 5294 (1974).
[13] I. P. Shkarofsky, T. W. Johnston, and M. P. Bachynski, *The Particle Kinetics of Plasmas* (Addison-Wesley, Reading, MA 1966).
[14] J. R. Albritton, Phys. Rev. Lett. **50**, 2078 (1983).
[15] N. R. Pereira and K. G. Whitney, Phys. Rev. A **38**, 319 (1988).
[16] P. E. Pulsifer and K. G. Whitney, NRL Memorandum Report No. 6662, 1990 (unpublished).
[17] I. P. Shkarofsky, Phys. Rev. Lett. **42**, 1342 (1979).
[18] T. W. Johnston and J. M. Dawson, Phys. Fluids **16**, 722 (1973).
[19] L. Spitzer, Jr., *Physics of Fully Ionized Gases* (Interscience, New York, 1962).
[20] S. I. Braginskii, in *Reviews of Plasma Physics,* edited by M. A. Leontovich (Consultants Bureau, New York, 1965), Vol. 1, p. 205.
[21] C. T. Dum, Phys. Fluids **21**, 945 (1978).
[22] P. Alaterre, J.-P. Matte, and M. Lamoureaux, Phys. Rev. A **34**, 1578 (1986).
[23] Patrick Mora and Hervé Yahi, Phys. Rev. A **26**, 2259 (1982).
[24] K. G. Whitney and P. E. Pulsifer, Phys. Rev. E **47**, 1968 (1993).
[25] J. N. Broughton and R. Fedosejevs, J. Appl. Phys. **74**, 3712 (1993).
[26] J. P. Matte, T. W. Johnston, J. Delettrez, and R. L. McCrory, Phys. Rev. Lett. **53**, 1461 (1984).